arXiv:0906.3390v1 [quant-ph] 18 Jun 2009

Experimental Test of Bell inequalities with Six-Qubit Graph States

Wei-Bo Gao,[1] Xing-Can Yao,[1] Ping Xu,[1] Otfried Gühne,[2, 3] Adán Cabello,[4]
Chao-Yang Lu,[1] Tao Yang,[1] Zeng-Bing Chen,[1] and Jian-Wei Pan[1, 5]
[1]*Hefei National Laboratory for Physical Sciences at Microscale and Department of Modern Physics, University of Science and Technology of China, Hefei, Anhui 230026, China*
[2]*Institut für Quantenoptik und Quanteninformation, Österreichische Akademie der Wissenschaften, Technikerstraße 21A, A-6020 Innsbruck, Austria*
[3]*Institut für theoretische Physik, Universität Innsbruck, Technikerstraße 25, A-6020 Innsbruck, Austria*
[4]*Departamento de Física Aplicada II, Universidad de Sevilla, E-41012 Sevilla, Spain*
[5]*Physikalisches Institut, Ruprecht-Karls-Universität Heidelberg, Philosophenweg 12, 69120 Heidelberg, Germany*

(Dated: June 18, 2009)

We report on the experimental realization of two different Bell inequality tests based on six-qubit linear-type and Y-shape graph states. For each of these states, the Bell inequalities tested are optimal in the sense that they provide the maximum violation among all Bell inequalities with stabilizing observables and possess the maximum resistance to noise.

PACS numbers: 03.65.Ud, 42.65.Lm, 03.67.Bg, 03.67.Mn

Introduction.—Graph states are basic resources for one-way quantum computation [1], quantum error-correction [2], and studying multiparticle entanglement [3]. Moreover, they provide a test-bed to investigate quantum nonlocality, that is, the inconsistency between local hidden variable (LHV) theories and quantum mechanics [4, 5, 6, 7, 8]. Considerable efforts have been devoted to designing different Bell inequalities for graph states with many particles. Here, the aim is to find inequalities with a high quantum mechanical violation, as this is related to the detection efficiency required to perform a loophole-free testing of Bell inequality; moreover, the Bell inequality with a higher violation is more robust against noise. In these studies it has turned out that for many kinds of graph states, the violation of local realism increases exponentially with the number of particles [7, 8]. Experimental Bell tests with four-qubit cluster or Greenberger-Horne-Zeilinger (GHZ) states, which are examples of graph states, have been reported recently [9, 10, 11, 12].

In this paper we report an experimental realization of two different Bell tests based on two types of six-qubit graph states—the linear-type one LC_6 and the Y-shape one Y_6. The states are produced using the polarization and the spatial modes of four photons. Such states are also called hyper-entangled states and can be generated with good quality and a high generation rate [11, 13, 14, 15, 16, 17, 18]. The two Bell inequalities tested in this paper are optimal in the sense that they provide the maximum violation among all Bell inequalities with stabilizing observables only. Remarkably, they give the same high violation of local realism as the six-qubit GHZ state with the Mermin inequality [7], but the violation for the LC_6 and the Y_6 state is more robust against decoherence.

State preparation.—Let us first recall the notion of graph states. A graph state $|G\rangle$ is specified by its stabilizer [3], i.e., a complete set of operators g_i of which it is the unique joint eigenstate, $g_i\,|G\rangle = |G\rangle$ for all i, where

$$g_i = X_i \bigotimes_{j\in N(i)} Z_j. \qquad (1)$$

Here, i is some vertex in a graph (see also Fig. 1a) and $N(i)$ denotes its neighborhood, that is, all vertices connected with i. Furthermore, X_i and Z_j denote the usual Pauli operators acting on qubits i or j.

The graphs corresponding to our graph states are given in Fig. 1a and the experimental setup is shown in Fig. 1b. First, we use spontaneous parametric down conversion [19, 20] to create one entangled photon pair $(|H\rangle_1|H\rangle_2 + |V\rangle_1|V\rangle_2)/\sqrt{2}$ and two single photons $|+\rangle = (|H\rangle + |V\rangle)/\sqrt{2}$, where H, V denote horizontal and vertical polarization, and 1, 2 label the spatial modes of the photons. By using operations similar to fusion-II gates between photons above [21], we generate a state in

$$\begin{aligned}|LC_4\rangle = \frac{1}{2}\big[\,&|H\rangle_1|H\rangle_3\,(|H\rangle_2|H\rangle_4 + |V\rangle_2|V\rangle_4)\\ &+|V\rangle_1|V\rangle_3\,(|H\rangle_2|H\rangle_4 - |V\rangle_2|V\rangle_4)\big],\end{aligned} \qquad (2)$$

which is equivalent to a 4-photon linear-type cluster state under local unitary transformations [22].

Based on the state $|LC_4\rangle$, another two qubits in spatial modes are added to construct the 6-qubit state. If a beam of photons enter a polarizing beam splitter (PBS), the H-polarized one will follow one path, while the V-polarized one will follow the other path. Here we define the first path as the photon's H' spatial mode, and the latter one as its V' spatial mode. After we apply two Hadamard (H) gates on photons 1 and 4, and place two PBSs in the outputs of them (see Fig. 1b), the whole state will be converted to

$$
\begin{aligned}
|LC_6\rangle = \frac{1}{\sqrt{8}}\Big\{&\left[|H\rangle_1 |H'\rangle_1 + |V\rangle_1 |V'\rangle_1\right] |H\rangle_3 \\
&\otimes \left[\,|+\rangle_2 |H\rangle_4 |H'\rangle_4 + |-\rangle_2 |V\rangle_4 |V'\rangle_4\,\right] \\
&+ \left[\,|H\rangle_1 |H'\rangle_1 - |V\rangle_1 |V'\rangle_1\,\right] |V\rangle_3 \\
&\otimes \left[\,|-\rangle_2 |H\rangle_4 |H'\rangle_4 + |+\rangle_2 |V\rangle_4 |V'\rangle_4\,\right]\Big\} \\
&= \frac{1}{\sqrt{8}}\Big\{\left[\,|0\rangle_5 |0\rangle_1 + |1\rangle_5 |1\rangle_1\,\right] |0\rangle_3 \otimes \left[\,|\tilde{0}\rangle_2 |0\rangle_4 |0\rangle_6 \right. \\
&\left. + |\tilde{1}\rangle_2 |1\rangle_4 |1\rangle_6\,\right] + \left[\,|0\rangle_5 |0\rangle_1 - |1\rangle_5 |1\rangle_1\,\right] |1\rangle_3 \\
&\otimes \left[\,|\tilde{1}\rangle_2 |0\rangle_4 |0\rangle_6 + |\tilde{0}\rangle_2 |1\rangle_4 |1\rangle_6\,\right]\Big\}, \qquad (3)
\end{aligned}
$$

where $|\pm\rangle = (|H\rangle \pm |V\rangle)/\sqrt{2}$, $|\tilde{0}\rangle = (|0\rangle + |1\rangle)/\sqrt{2}$, and $|\tilde{1}\rangle = (|0\rangle - |1\rangle)/\sqrt{2}$. $|LC_6\rangle$ is equivalent to a 6-qubit linear-type graph state up to single qubit unitary transformations.

To prepare $|Y_6\rangle$ based on $|LC_4\rangle$, H gates are applied on photons 2 and 4, then photons 1 and 4 are transmitted through PBSs, and finally the whole state will be converted to

$$
\begin{aligned}
|Y_6\rangle = \frac{1}{2}\{\, &|H\rangle_1 |H\rangle_3 |H\rangle_2 |H\rangle_4 |H'\rangle_1 |H'\rangle_4 + |H\rangle_1 |H\rangle_3 \\
&|V\rangle_2 |V\rangle_4 |H'\rangle_1 |V'\rangle_4 + |V\rangle_1 |V\rangle_3 |H\rangle_2 |V\rangle_4 |V'\rangle_1 |V'\rangle_4 \\
&+ |V\rangle_1 |V\rangle_3 |V\rangle_2 |H\rangle_4 |V'\rangle_1 |H'\rangle_4 \,\} \qquad (4) \\
= \frac{1}{2}\{\, &|0\rangle_1 |0\rangle_3 |0\rangle_2 |0\rangle_4 |0\rangle_5 |0\rangle_6 + |0\rangle_1 |0\rangle_3 |1\rangle_2 |1\rangle_4 |0\rangle_5 |1\rangle_6 \\
&+ |1\rangle_1 |1\rangle_3 |0\rangle_2 |1\rangle_4 |1\rangle_5 |1\rangle_6 + |1\rangle_1 |1\rangle_3 |1\rangle_2 |0\rangle_4 |1\rangle_5 |0\rangle_6\}.
\end{aligned}
$$

This is equivalent to a Y-shape 6-qubit graph state up to single qubit unitary transformations.

Local measurements.—In order to measure the states' fidelities and test the Bell inequalities, we need to implement the desired local measurements. The measurement setups are shown in Fig. 1c, which is similar to Refs. [11, 16]. Here and in the following, x, y, z refer to the Pauli matrices for the spatial modes, and X, Y, Z refer to the Pauli matrices of the polarization modes. The measurements of x, y observables are implemented by overlapping different modes of a photon on a beam splitter (BS), and the measurement of z observable is implemented by blocking one or the other input path of the BS. The observables of polarization qubits are measured by placing a combination of a quarter-wave plate, a half-wave plate and a PBS in front of the single-photon detectors. Although a photon's polarization and spatial information is read out simultaneously, they are independent measurements and have no influence on each other.

The measurements of spatial modes require single photon interferometers as shown Fig. 2a. This interferometer is very easily affected by its environment and can only be stable for a few minutes. In our experiment, an ultra-stable Sagnac-ring technique [23, 24] is applied to satisfy the required stability. First, we design a crystal combining a PBS and a BS as shown in Fig. 2c. Then, we construct the single photon interferometer in a Sagnac-ring configuration (see Fig. 2b). The H-polarized component is transmitted and propagated through the interferometer in the counterclockwise direction, while the V-polarized component is reflected and propagated through the interferometer in the clockwise direction. Then, the interference happens when the two components meet at the BS. Such interferometer can be stable for at least ten hours [18].

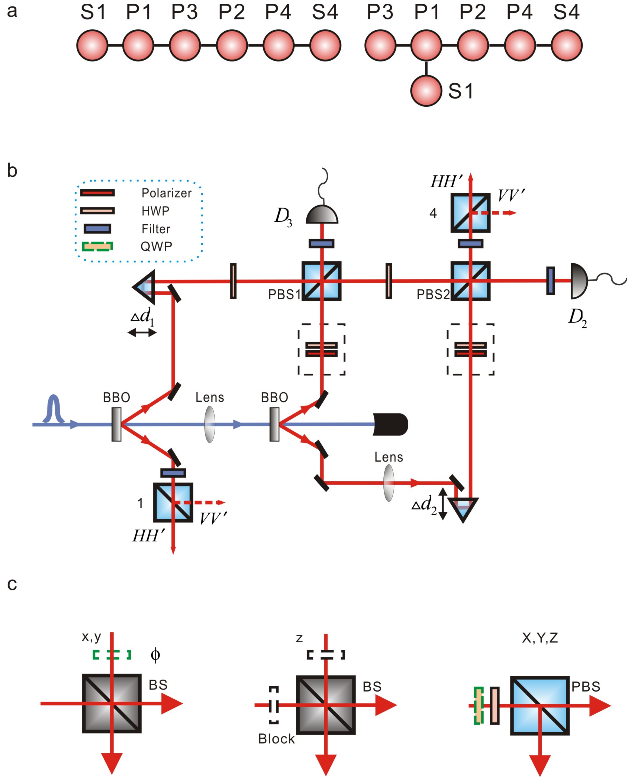

FIG. 1: **a**. The two created graph states. P_i represents (polarization) qubit i, and S1 and S4 represent (spatial) qubits 5 and 6, respectively. **b**. Scheme of the experimental setup to generate the desired graph states. Femtosecond laser pulses (≈ 200 fs, 76 MHz, 788 nm) are converted to ultraviolet and transmitted through two BBO crystals (2 mm), where two photon pairs are generated. The observed two-fold coincident count rate is about 2.6×10^4/s. Two additional polarizers are inserted into the arms of the second pair to prepare two single photon states. **c**. The measurement setups for the desired observables. The first setup is for x measurement of spatial qubits when $\phi = 0$, and for y measurement of spatial qubits when $\phi = 90°$. The second one is for z measurement of spatial qubits by using blocks in the two paths of the beam splitter. The third one is for X, Y, Z measurements of polarization qubits by using half wave plates (HWPs), quarter wave plates (QWPs), and PBSs.

Fidelity.—To estimate the fidelity of the prepared states, we consider an observable B with the property $\langle\phi|\, B\, |\phi\rangle \leq \langle\phi|LC_6\rangle\langle LC_6|\phi\rangle = F_{LC_6}$ for any $|\phi\rangle$. This

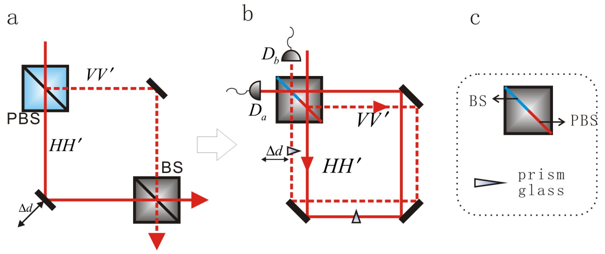

FIG. 2: Apparatuses of constructing Sagnac-ring interferometer in order to measure all the necessary observables of spatial modes. **a**. The original scheme of single photon interferometer, which is easily affected by the environment and can be stable for only several minutes. **b**. Our single photon interferometer in the Sagnac-ring model. Two special prism glasses are inserted to change optical path delay in order to obtain the desired phase. **c**. A special crystal combining the function of beam splitter and PBS.

means $\langle B\rangle_{\text{exp}}$ is a lower bound of the fidelity of the experimentally produced state [25]. The actual B for the LC$_6$ state is given in Ref. [26]. We obtained the result

$$F_{LC_6} \geq \langle B\rangle_{\text{exp}} = 0.61 \pm 0.01, \tag{5}$$

clearly exceeding 1/2, also proving the genuine 6-qubit entanglement of that state [25].

As explained in Ref. [27], for the Y$_6$-state there is also an observable B such that

$$\langle B\rangle_{\text{exp}} \leqslant \text{tr}(|Y_6\rangle\langle Y_6|\,\rho_{\text{exp}}) = F_{Y_6}, \tag{6}$$

so $\langle B\rangle_{\text{exp}}$ is the lower bound on the fidelity. Experimentally, we find $\langle B\rangle_{\text{exp}} = 0.63 \pm 0.04 > 1/2$, giving again clear evidence of genuine 6-qubit entanglement.

Optimal Bell inequalities.—The optimal Bell inequality (i.e., the one having the highest resistance to noise) involving only stabilizing observables for the LC$_6$ state in the form of Eq. (3) is

$$\langle \mathcal{B}_{LC6}\rangle = \langle (\mathbb{1}+g_5)g_1(\mathbb{1}+g_3)(\mathbb{1}+g_2)g_4(\mathbb{1}+g_6)\rangle \leq 4, \tag{7}$$

where $g_5 = z_5Z_1$, $g_1 = x_5X_1Z_3$, $g_3 = Z_1X_3Z_2$, $g_2 = Z_3X_2Z_4$, $g_4 = Z_2X_4x_6$ and $g_6 = Z_4z_6$ [6]. These g_i are stabilizing operators of the linear-type graph state, i.e. the graph state is an eigenstate of all the g_i with eigenvalue $+1$, as one can easily check. To obtain the required measurements for the Bell test, one just has to consider each of the 16 terms separately, which arise from multiplying out $\mathcal{B}_{LC6}$ (see Table I). As all these terms are products of stabilizing operators, the cluster state is an eigenstate of all these terms, and the value for the ideal cluster state is the algebraic maximum $\langle \mathcal{B}_{LC6}\rangle = 16$.

Similarly, the optimal stabilizer Bell inequality for the Y$_6$ state is [6]

$$\langle \mathcal{B}_{Y6}\rangle = \langle (\mathbb{1}+g_3)g_1(\mathbb{1}+g_5)(\mathbb{1}+g_2)g_4(\mathbb{1}+g_6)\rangle \leq 4, \tag{8}$$

Observable	Value	Observable	Value
$xXZZXx$	0.61 ± 0.04	$-xXZZYy$	0.60 ± 0.04
$xXIYYx$	0.63 ± 0.04	$xXIYXy$	0.62 ± 0.04
$-yYZZXx$	0.55 ± 0.04	$yYZZYy$	0.56 ± 0.04
$-yYIYYx$	0.65 ± 0.03	$-yYIYXy$	0.56 ± 0.04
$xYYIXx$	0.58 ± 0.04	$-xYYIYy$	0.63 ± 0.04
$xYXXYx$	0.58 ± 0.04	$xYXXXy$	0.60 ± 0.04
$yXYIXx$	0.55 ± 0.04	$-yXYIYy$	0.56 ± 0.04
$yXXXYx$	0.57 ± 0.04	$yXXXXy$	0.60 ± 0.04

TABLE I: Experimental values of the observables on $|LC_6\rangle$ required in the test of the optimal Bell inequality. Each experimental value is obtained by measuring in an average time of 400 seconds and considers the Poissonian counting statistics of the raw detection events for the experimental errors. The order of the qubits is 5-1-3-2-4-6.

where now $g_3 = Z_1Z_3$, $g_1 = X_1X_3X_2x_5$, $g_5 = Z_1z_5$, $g_2 = Z_1Z_2Z_4$, $g_4 = Z_2Z_4z_6$, and $g_6 = Z_4z_6$. Again, the value for the pure Y$_6$ state is $\langle \mathcal{B}_{Y6}\rangle = 16$.

A remarkable feature of these Bell inequalities is that the LC$_6$ state and the Y$_6$ state violate local realism by a factor of four, which is also the violation for the six-qubit GHZ state, if only stabilizing elements are considered (the optimal Bell inequality is then the Mermin inequality [6]). However, the LC$_6$ and Y$_6$ state are more resistant to decoherence than the GHZ$_6$ [28]. In fact, one can directly see that if decoherence acts as a depolarizing channel on each qubit, the violation of the Mermin inequality for the GHZ$_6$ state decreases faster than for the graph states considered here. Namely, if noise like $\varrho \mapsto p\varrho + (1-p)\mathbb{1}/2$ is acting on each qubit separately, the value of the Mermin inequality decreases with p^6, as the Mermin inequality consists only of full correlation terms. In our Bell inequalities, however, half of the terms contain the identity on one qubit (see Tables I and II), which means that they decay only with p^5, and the total violation decreases like $(p^6 + p^5)/2$.

This proves that the non-locality vs. decoherence ratio of GHZ states is not universal: there are states with a similar violation which are more robust against decoherence. This result indicates that Bell inequalities for graph states have promising advantages towards observing macroscopic violations of Bell inequalities [7].

The experimental results are given in Tables I and II. From these data we find

$$\begin{aligned} \langle \mathcal{B}_{LC6}\rangle_{\text{exp}} &= 9.40 \pm 0.16, \\ \langle \mathcal{B}_{Y6}\rangle_{\text{exp}} &= 9.30 \pm 0.17, \end{aligned} \tag{9}$$

which violate the classical bound by 34 and 31 standard deviations.

Let us consider the ratio $\mathcal{D}$ between the quantum value of the Bell operator and its bound in LHV theories. This is related to the detection efficiency required to perform a

Observable	Value	Observable	Value
$-XXIYxy$	0.62 ± 0.04	$XYIYyy$	0.59 ± 0.05
$YYIYxy$	0.58 ± 0.05	$YXIYyy$	0.61 ± 0.05
$XXIXxx$	0.56 ± 0.04	$-XYIXyx$	0.54 ± 0.04
$-YYIXxx$	0.61 ± 0.04	$-YXIXyx$	0.63 ± 0.04
$-YXZXxy$	0.57 ± 0.05	$YYZXyy$	0.62 ± 0.04
$-XYZXxy$	0.55 ± 0.04	$-XXZXyy$	0.58 ± 0.04
$-YXZYxx$	0.54 ± 0.04	$YYZYyx$	0.57 ± 0.05
$-XYZYxx$	0.59 ± 0.04	$-XXZYyx$	0.54 ± 0.04

TABLE II: Experimental values of all the observables on $|Y_6\rangle$ for the optimal Bell inequality measurement. Each experimental value is obtained by measuring in an average time of 400 seconds and propagated Poissonian statistics of the raw detection events is also considered. The order of the qubits is 1-3-2-4-5-6.

loophole-free testing of Bell inequality and if $\mathcal{D}$ increases, the required detection efficiency decreases [29]. Experimentally, we have

$$\begin{aligned} \mathcal{D}_{LC6} = \langle \mathcal{B}_{LC6} \rangle_{\rm exp} / \langle \mathcal{B}_{LC6} \rangle_{\rm LHV} &= 2.35 \pm 0.04, \\ \mathcal{D}_{Y6} = \langle \mathcal{B}_{Y6} \rangle_{\rm exp} / \langle \mathcal{B}_{Y6} \rangle_{\rm LHV} &= 2.33 \pm 0.04. \end{aligned} \quad (10)$$

These are larger values compared to previous experiments with similar Bell inequalities for four-qubit cluster states, where values of $\mathcal{D}$ from 1.29 to 1.70 have been achieved [9, 10, 11]; using a Bell inequality with non-stabilizer observables for the four-qubit GHZ state, $\mathcal{D} = 2.22$ has been reached [12]. Therefore, despite of having a lower fidelity than in the four-qubit experiments, we find a higher violation of local realism, which demonstrates that the amount of nonlocality can increase with the number of qubits.

Conclusion.—We have implemented two multi-qubit Bell tests on two six-qubit graph states. These states under consideration show the same violation of local realism as the GHZ states, however, they are more robust to decoherence. This rises several open questions for further investigations: From a theoretical point of view, it is interesting to investigate the relationship between decoherence and nonlocality further. The aim is to characterize states, which show a high violation of local realism, while being still robust against decoherence. From the experimental side, it would be of great interest to generate states which are assumed to be robust against decoherence and to observe the predicted decay behavior of entanglement.

This work is supported by the NNSF of China, the CAS, and the National Fundamental Research Program (under Grant No. 2006CB921900). OG acknowledges support from the FWF (START prize) and the EU (OLAQUI, SCALA, and QICS). AC acknowledges support by the projects No. P06-FQM-02243 and No. FIS2008-05596.

[1] R. Raussendorf and H.J. Briegel, Phys. Rev. Lett. **86**, 5188 (2001); M. van den Nest *et al.*, Phys. Rev. Lett. **97**, 150504 (2006).
[2] D. Schlingemann and R.F. Werner, Phys. Rev. A **65**, 1, 012308 (2002); D. Schlingemann, Quantum Inf. Comput. **2**, 307 (2002).
[3] M. Hein, J. Eisert, and H.J. Briegel, Phys. Rev. A **69**, 062311 (2004); M. Hein *et al.*, in *Quantum Computers, Algorithms and Chaos*, edited by G. Casati, D.L. Shepelyansky, P. Zoller, and G. Benenti (IOS Press, Amsterdam, 2006), quant-ph/0602096.
[4] V. Scarani *et al.*, Phys. Rev. A **71**, 042325 (2005); J. Barrett *et al.*, Phys. Rev. A **75**, 012103 (2007); O. Gühne and A. Cabello, Phys. Rev. A **77**, 032108 (2008).
[5] A. Cabello and P. Moreno, Phys. Rev. Lett. **99**, 220402 (2007).
[6] A. Cabello, O. Gühne, and D. Rodríguez, Phys. Rev. A **77**, 062106 (2008).
[7] N.D. Mermin, Phys. Rev. Lett. **65**, 1838 (1990).
[8] O. Gühne *et al.*, Phys. Rev. Lett. **95**, 120405 (2005); G. Tóth, O. Gühne, and H.J. Briegel, Phys. Rev. A **73**, 022303 (2006); L.-Y. Hsu, Phys. Rev. A **73**, 042308 (2006).
[9] P. Walther, M. Aspelmeyer, K. J. Resch, and A. Zeilinger, Phys. Rev. Lett. **95**, 020403 (2005).
[10] N. Kiesel, *et al.*, Phys. Rev. Lett. **95**, 210502 (2005).
[11] G. Vallone *et al.*, Phys. Rev. Lett. **98**, 180502 (2007).
[12] Z. Zhao *et al.*, Phys. Rev. Lett. **91**, 180401 (2003).
[13] P. G. Kwiat, J. Mod. Opt. **44**, 2173 (1997).
[14] J. T. Barreiro *et al.*, Phys. Rev. Lett. **95**, 260501 (2005).
[15] G. Vallone *et al.*, Phys. Rev. Lett. **100**, 160502 (2008).
[16] K. Chen *et al.*, Phys. Rev. Lett. **99**, 120503 (2007).
[17] H. S. Park *et al.*, Optics Express **15**, 17960 (2007).
[18] W.-B. Gao *et al.*, arXiv:0809.4277.
[19] P.G. Kwiat *et al.*, Phys. Rev. Lett. **75**, 4337 (1995).
[20] Z. Zhao *et al.*, Nature (London) **430**, 54 (2004).
[21] D.E. Browne and T. Rudolph, Phys. Rev. Lett. **95**, 010501 (2005).
[22] Y. Tokunaga *et al.*, Phys. Rev. Lett. **100**, 210501 (2008).
[23] T. Nagata *et al.*, Science **316**, 726 (2007).
[24] M.P. Almeida *et al.*, Science **319**, 579 (2007).
[25] O. Gühne and G. Tóth, Phys. Rep. **474**, 1 (2009).
[26] W.-B. Gao *et al.*, arXiv:0905.2103.
[27] See the online material of C.-Y. Lu *et al.*, Phys. Rev. Lett. **102**, 030502 (2009).
[28] W. Dür and H.-J. Briegel, Phys. Rev. Lett. **92**, 180403 (2004).
[29] A. Cabello, D. Rodríguez, and I. Villanueva, Phys. Rev. Lett. **101**, 120402 (2008).